Fault Diagnosis of Harmonic Drive With Imbalanced Data Using Generative Adversarial Network

Guo Yang, Yong Zhong, *Member, IEEE*, Lie Yang, Hui Tao, Jianying Li, and Ruxu Du

***Abstract*— Harmonic drive is the core component of the industrial robot, and its fault diagnosis is crucial to the reliability and performance of the equipment. Most machine learning methods achieve good results based on the assumption of data balance. However, the scarce fault data of harmonic drive is difficult to collect, resulting in various imbalanced health status samples, which has an adverse effect on fault diagnosis. In this article, we propose a data generation method based on generative adversarial networks (GANs) to solve the problem of data imbalance and utilize the multiscale convolutional neural network (MSCNN) to realize the fault diagnosis of the harmonic drive. First, the data collected from three vibration acceleration sensors are preprocessed by fast Fourier transform (FFT) to obtain the frequency spectrum of the vibration signal. Second, multiple GANs were adopted to generate various fault spectrum data and the data selection module (DSM) is elaborately designed to filter and purify these data. Third, the filtered generated data will be combined with the real data to form a balanced dataset, and then the MSCNN is used to achieve multiclassification of the health status of the harmonic drive. Finally, the experiments have been implemented on an industrial robot vibration test bench to validate the effectiveness of our approach. The results have shown the fault multiclassification accuracy as 98.49% under imbalanced fault data conditions, which outperforms that of the other compared methods.**

***Index Terms*— Data selection module (DSM), fault diagnosis, generative adversarial network (GAN), harmonic drive, imbalanced data, multiscale convolutional neural network (MSCNN).**

I. Introduction

HARMONIC drives are indispensable transmission parts of industrial robots, which have the advantage of compact structure, lightweight, small size, large reduction ratio, high transmission accuracy, high efficiency, and high rigidity [1]. The harmonic drive is adversely affected by manufacturing and assembly errors and depends on operating conditions due to its complex design. Besides, it is a highly nonlinear system and usually coupled with other external electromechanical components, therefore the vibration signals usually exhibit multiscale characteristics. Moreover, the fault categories of the harmonic drive are complex and diverse, and the fault data are scarce, which leads to various categories of imbalanced health status data. Therefore, it adversely affects the diagnostic performance of the harmonic drives.

However, the current fault diagnosis of the harmonic drive usually relies on simple spectrum instruments and the technical experience, and the accuracy and efficiency are low. Moreover, there is little research on the entire harmonic drive and it is difficult to obtain ideal results [2]. Only limited literature focuses on the fault diagnosis of its components (flexspline or flexible bearings) [3]–[5]. Therefore, it is urgent to propose an effective intelligent method to improve the fault diagnosis accuracy of harmonic drive in shopfloor applications.

There are many mature machine learning methods for fault monitoring and diagnosis of rotating machinery equipment (excluding harmonic drives), such as the convolutional neural network (CNN), deep belief network (DBN), and recurrent neural network (RNN). For example, in [6]–[8], various intelligent methods all have achieved good classification performance in rolling element bearings fault classification. However, the premise for the above methods to obtain the ideal results is a large number of balanced samples of different categories. Therefore, the biggest problem facing rotating machinery in fault diagnosis is data imbalance of various categories caused by scarce fault data samples [9].

Fig. 1 describes the proportion of various categories of health status data of harmonic drive, reflecting the true fault attributes of the product. It reveals that the amount of fault data for different categories is different, and they are all much smaller than normal data. The existing fault diagnosis methods for harmonic drive do not consider the problem of data imbalance, which will adversely affect the classification performance of most machine learning methods [10]. The common methods to address this problem include [11]: improved loss function methods, improved models, and data augmentation approaches. For example, He *et al.* [12] adopted the multiscale neural network with focal loss (MNN-FC) to achieve the fault diagnosis of wind turbines under data imbalance.

Manuscript received March 23, 2021; revised May 23, 2021; accepted May 25, 2021. Date of publication June 14, 2021; date of current version June 25, 2021. This work was supported in part by the Strategic Priority Research Program of the Chinese Academy of Sciences (Class A) under Grant XDA22040203, in part by the Opening Project of National and Local Joint Engineering Research Center for Industrial Friction and Lubrication Technology under Grant 2021-GD-0005, and in part by the Natural Science Foundation of Guangdong Province under Grant 2020A1515010621. The Associate Editor coordinating the review process was Shibin Wang. *(Corresponding author: Yong Zhong.)*

Guo Yang, Yong Zhong, Lie Yang, and Ruxu Du are with the Shien-Ming Wu School of Intelligent Engineering, South China University of Technology, Guangzhou 511442, China (e-mail: 1318458639@qq.com; zhongyong@scut.edu.cn; 201810100415@mail.scut.edu.cn; duruxu@scut.edu.cn).

Hui Tao is with the Shien-Ming Wu School of Intelligent Engineering, South China University of Technology, Guangzhou 511442, China, and also with the National and Local Joint Engineering Research Center for Industrial Friction and Lubrication Technology, Guangzhou 510700, China (e-mail: taohui06@163.com).

Jianying Li is with the School of Mechanical and Automotive Engineering, Zhaoqing University, Zhaoqing 526061, China (e-mail: 360103919@qq.com).

Digital Object Identifier 10.1109/TIM.2021.3089240

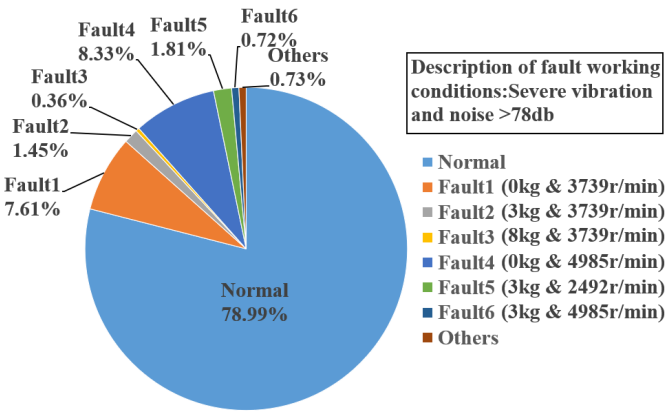

Fig. 1. Proportion of various health status data of harmonic drive.

Ng *et al.* [13] proposed a cost-sensitive stochastic sensitivity measure to weight the full available samples of different classes in electricity pricing binary classification. However, these deep learning methods do not augment the imbalanced training data. The serious imbalance in the number of samples caused by various categories of scarce fault data will adversely affect the performance of the network [14]. Random undersampling and oversampling techniques are widely used in data preprocessing to achieve data balance [15]. For example, Han *et al.* [16] used oversampling technology based on synthetic minority oversampling technology (SMOTE) to randomly synthesize minority classes. In [17] and [18], the synthetic oversampling technique "adaptive synthetic sampling approach (ADASYN)" and its improved method called modified ADASYN were proposed to linearly interpolate virtual data into the dataset separately. However, the samples generated by these methods based on adjacent data interpolation cannot provide enough new useful information, and the sample diversity is insufficient.

Recently, generative adversarial networks (GANs) have been applied to data augmentation fields since they can effectively learn the basic distribution of the real data and generate more realistic data to expand the training datasets [19]. The original GAN and its variants have been used to generate data in imbalanced learning [20]–[22]. For example, GAN is used to oversample the original dataset, and then use a deep neural network (DNN) to realize the fault diagnosis of induction motor [20]. The conditional generative adversarial network (CGAN) is used to generate minority category data, and the quality of the data has been significantly improved [21]. The auxiliary classifier generative adversarial (ACGAN) is designed for signal generation to achieve the machine fault diagnosis [22]. Huang *et al.* [23] presented an unsupervised image-to-image translation framework that can allow users to control the style of translation outputs by providing a style image. Although some models (such as conditional GAN, etc.) can generate different kinds of data at the same time, it is suggested to use multiple GANs in the study of 1-D fault vibration signals, which can better learn the fault characteristics of each category [24]. Moreover, the shortcoming of GANs is that the training process is unstable [25], resulting in randomly generated data and part of that does not conform to the real data distribution. Therefore, these methods mentioned above failed to achieve the optimal results and lack an effective technique to postprocess the randomly generated data.

To tackle the imbalanced fault data problem of harmonic drive, we propose an intelligent fault diagnosis framework called GAN-data selection module (DSM)-multiscale convolutional neural network (MSCNN) to effectively augment various categories of fault data and realize the fault diagnosis of the harmonic drive. First, the frequency spectrum of the vibration acceleration signals collected by multiple sensors are obtained through fast Fourier transform (FFT). Second, multiple GANs were used to augment various categories of fault spectrum data, and the DSM composed of Mahalanobis distance and Euclidean distance is designed to filter and purify the generated rough data to select high-quality generated data. Third, the various categories of generated data with real data distribution characteristics and the real data were used to construct the balanced dataset for subsequent training. Finally, MSCNN is designed to effectively obtain the multiscale features of the signal, and simultaneously realize the multiclassification of the health status of the harmonic drive. The experimental results show that the proposed method is effective to improve the fault diagnosis performance of the harmonic drive with imbalanced fault data. The main contributions of this article are as follows.

1) We designed a postprocessing module that used the Mahalanobis distance and Euclidean distance to filter and purify the rough generated data, respectively. It can obtain the high-quality generated data with real characteristic distribution and can effectively solve the problem of unstable generated samples from GANs.
2) We proposed an effective intelligent fault diagnosis method: GAN-DSM-MSCNN architecture, which can effectively capture the complementary and inherent features in the harmonic drive vibration signal and significantly improve the performance of multiclassification. It has shown broad prospects in practical applications.

The contents of the subsequent sections of this article are as follows. Section II details the mechanical structure of the harmonic drive and the proposed fault diagnosis method. Section III shows the experimental platform, the health status dataset, and the parameters of the network. Section IV shows the generated data, the accuracy of multiclassifications, and the impact of different data imbalance ratios and various classifiers on diagnostic performance. Finally, Section V gives the conclusion of the work and prospects.

II. Materials and Methods

A. Mechanical Structure of Harmonic Drive

The harmonic drive is a special type of transmission mechanism that relies on elastic deformation to realize harmonic transmission. The example of a mechanical structure of the LHSG-17-100-C-IV-2 model harmonic drive is given in Fig. 2.

Harmonic drive mainly includes the wave generator (including cam and flexible bearing), flexspline, and circular spline. The wave generator is used as the input of the harmonic drive,

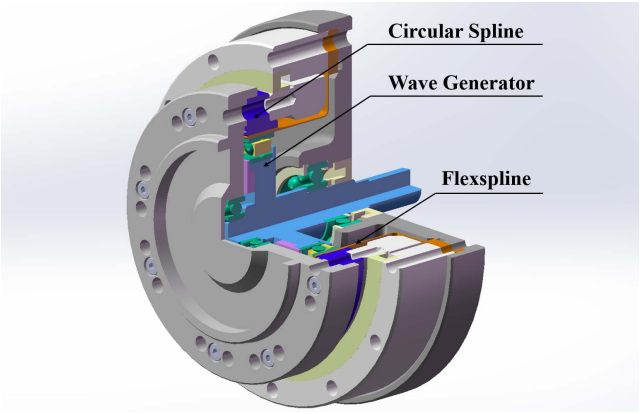

Fig. 2. Mechanical structure of LHSG-17-100-C-IV-2 model.

the cam is fixed to the motor shaft, and the flexible bearing is connected to the inner ring of the flexspline. The outer ring of the flexspline is fixed on the body of the harmonic drive. The gears between the flexspline and the circular spline are not completely meshed, and the circular spline is used as the power output. The flexible bearing of the wave generator relies on elastic deformation to drive the circular spline to move to achieve the purpose of transmission. The number of teeth of the flexspline and the circular spline is 200 and 202, respectively.

B. GAN-DSM-MSCNN Architecture

The goal of GAN-DSM-MSCNN is to effectively realize the fault diagnosis of the harmonic drive by generating various types of fault data and constructing a balanced training dataset. The architecture mainly consists of four stages (shown in Fig. 3). In stage 1, the vibration signal of the harmonic drive is collected through three acceleration sensors, and then FFT is used to obtain the spectrum of the original signal. Besides, the data is normalized to construct the original dataset for subsequent data generation. In stage 2, multiple GANs in which the network consists of convolutional layer and fully connected layer are used to generate various types of scarce fault data of the harmonic drive. In stage 3, the DSM (including data filtering and data purification) is designed to filter and purify the generated data, which can select the high-quality generated data. In stage 4, real samples and various types of generated fault samples are used to form a balanced training set, and then MSCNN (including multiscale decomposition and 2-D-CNN) is used to implement fault multiclassification of harmonic drivers.

1) Data Preprocessing: In stage 1, three acceleration sensors installed at the end of the robot in orthogonal directions are used to collect the vibration signal of the harmonic drive, and then these signals are resampled to four times the original number by moving a fixed sampling window. Subsequently, the FFT technique is used to process the resampled vibration signals to obtain the original spectrum dataset for subsequent data generation and fault diagnosis. Then, each sample is stacked as a grayscale bitmap with a pixel range of 0–255 according to (1), which serves as the input of the network. Besides, these data will be further normalized to 0–1 according to (2) to accelerate the convergence speed of network training. The Value represents each data value on the signal, and Range is the maximum value of the signal

$$\text{Result} = \frac{255 \times (\text{Value} + \text{Range})}{2 \times \text{Range}} \tag{1}$$

$$\text{scaled value} = \frac{\text{value} \times 2}{255} - 1. \tag{2}$$

2) Data Generation: In stage 2, each GAN (including a pair of a generator and a discriminator) is used to generate one type of 1-D fault data for subsequent data selection. Besides, N generative models with the same network structure are used to generate N scarce fault data categories, as shown in Fig. 4.

The objective function of the GAN model for each type of fault data can be simplified to the following formula:

$$\min_{\theta_g} \max_{\theta_d} V(\theta_d, \theta_g) = E_{x\sim p(x)}[\log(D(x))] + E_{z\sim p(z)}[\log(1 - D(G(z)))]. \tag{3}$$

In the training process of GAN, the discriminator is used to distinguish the true or false of each input, and it updates the gradient by increasing the stochastic gradient according to the following formula. Therefore, the discriminating ability of the discriminator will gradually be enhanced

$$\nabla\theta_d \frac{1}{m} \sum_{i=1}^{m} [\log(D(x^{(i)})) + \log(1 - D(G(z^{(i)})))]. \tag{4}$$

Meanwhile, the gradients of each generator will be updated by reducing the stochastic gradient according to the following formula. Therefore, the generator's ability to generate data will also become stronger, and the generated data will be more deceptive and difficult to distinguish

$$\nabla\theta_g \frac{1}{m} \sum_{i=1}^{m} \log(1 - D(G(z^{(i)}))). \tag{5}$$

Finally, each discriminator D will converge to the optimal output according to the following formula. Therefore, we can further obtain N categories of fault data with real data distribution through the training of N generators and N discriminators

$$D^*(x) = \frac{p_{\text{data}}(x)}{p_{\text{data}}(x) + p_g(z)}. \tag{6}$$

It should be particularly pointed out that the parameters of GAN are difficult to debug to achieve good results, and the detailed parameters will be given in Section III. Besides, the discriminator of our proposed network is composed of a CNN module, which can effectively extract deep features. Moreover, data rolling and averaging operations are also used to adjust various categories and different numbers of generated fault samples.

3) Data Selection: In stage 3, the DSM is elaborately designed as a postprocessing technique to filter and purify the raw generated data, which can help to select the generated data that conforms to the real data distribution and effectively solve the problem of unstable samples generated by GANs.

First, Mahalanobis distance [26] is used as a measurement to initially filter randomly generated data that is not within

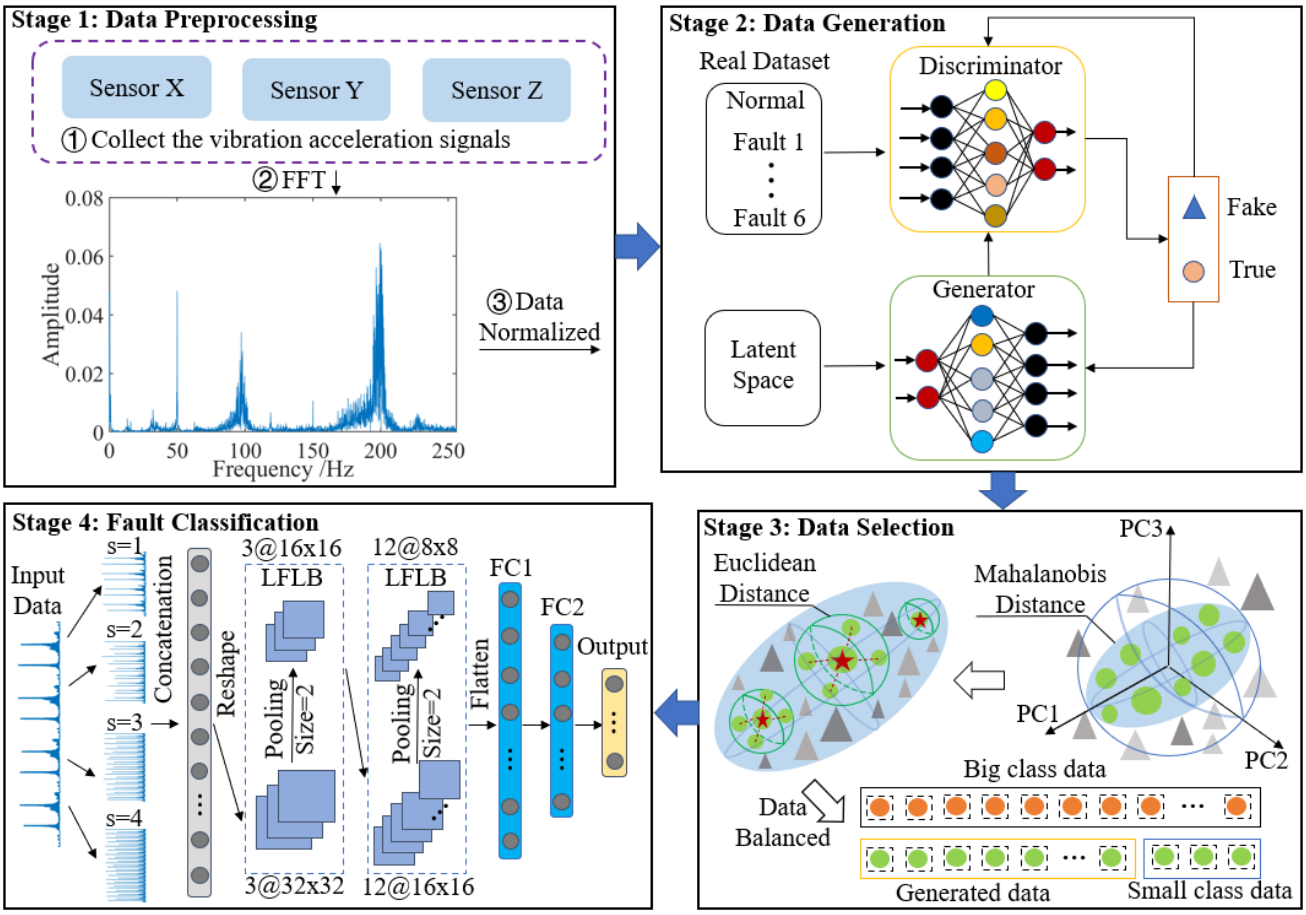

Fig. 3. Architecture of the GAN-DSM-MSCNN.

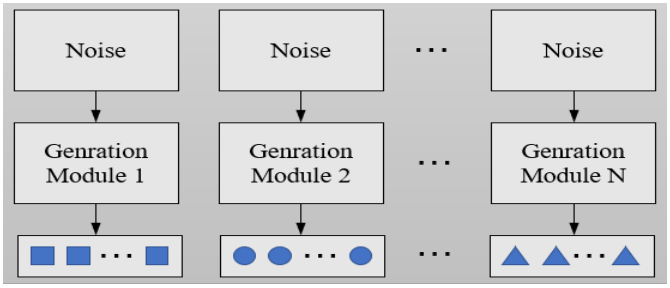

Fig. 4. Frame of multiple generation modules.

the distribution range of the real data, and it can consider the importance of data in different dimensions. For example, γ th represents the ith category in the real datasets $S_\gamma = (S_{\gamma\_1}, S_{\gamma\_2}, \ldots, S_{\gamma\_m})$, $\gamma = (1, 2, \ldots, N)$, including m categories. Besides, $\bar{S}_\gamma$ is the average value of each dimension of the actual datasets and represents the center in this dimension. Therefore, the Mahalanobis distance between S_{γ_i} $(i = (1, 2, \ldots, m))$ and S_γ is calculated as follows:

$$\mathrm{MD}(S_{\gamma\_i}, S_\gamma) = \sqrt{(S_{\gamma\_i} - \overline{S_\gamma})' \mathrm{cov}(S_\gamma)^{-1} (S_{\gamma\_i} - \overline{S_\gamma})} \quad (7)$$

where the covariance matrix $\mathrm{cov}(S_\gamma)$ requires inverse. Besides, the principal component analysis (PCA) technique is a technique for data dimensionality reduction, which can be used to set the minimum real data distribution space to eliminate generated data that is not within this range. Data dimensionality reduction not only can intuitively see the difference between actual data and generated data but also can indirectly reflect the performance of the generated network model.

Second, the Euclidean distance [27] is used to further purify the data generated in the sample space range selected in the previous step. The formula for calculating the Euclidean distance between point y_1 and point y_2 is given as follows:

$$\mathrm{ED}(y_1, y_2) = \|y_1 - y_2\|_2 = \sqrt{\sum_{k=1}^{u} (y_1 - y_2)^2} \quad (8)$$

where u represents the total dimensionality of the data point. After these two postprocessing steps, the filtered high-quality generated data will be retained to construct a balanced dataset for subsequent training.

4) Fault Classification: In stage 4, the multiscale decomposition module is designed to obtain the complementary and inherent characteristics of the signals at various scales [28]. For example, x_i is the ith value of the original signal $x = \{x_1, x_2, \ldots, x_N\}$, with N samples in total. The continuous signal $\{y^{(s)}\}$ is obtained by performing operations on the original signal with different scales s. Then, four-layer scale

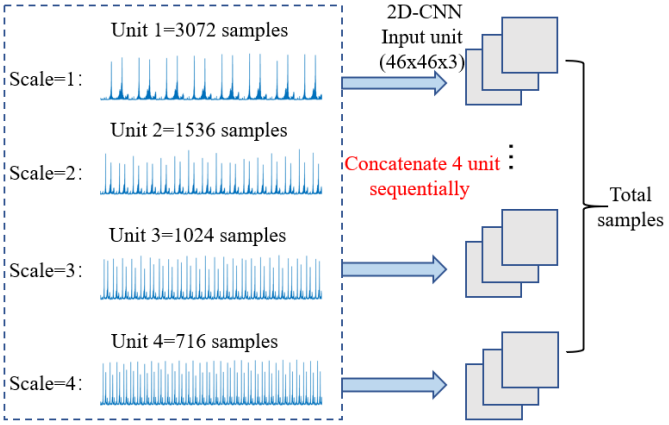

Fig. 5. Process of fusion of multiscale signals into 2-D-CNN units.

decomposition was used in this article, and the calculation of each element of different scale signals is as follows:

$$y_j^{(s)} = \frac{1}{s} \sum_{i=(j-1)s+1}^{js} x_i, \quad 1 \le j \le \frac{N}{s}. \tag{9}$$

According to the input unit size of the convolutional network and the multiscale factor coefficients, the signals of the above four scales will be intercepted 3072, 1536, 1024, 716 continuous data separately to form each unit, and then these four units will concatenate sequentially to construct each 2-D-CNN input unit for subsequent CNN training. The process of data fusion and conversion of various scale signals into a 2-D-CNN input unit is given in Fig. 5.

Besides, the calculation of the signal-to-noise ratio (SNR) is shown in the following formula. The original test samples were used mixed with the Gaussian noise to evaluate the influence of external environmental noise on fault diagnosis

$$\mathrm{SNR(dB)} = 10 \times \log_{10}^{(P_{\mathrm{signal}}/P_{\mathrm{noise}})} \tag{10}$$

where P_{signal} and P_{noise} represent the power of the original vibration samples and the vibration samples that contains the Gaussian noise, respectively.

III. Experiments

A. Setup and Data Collection

The industrial robot vibration test experimental bench contains an industrial robot, harmonic drives, the vibration analyzer [Svenska Kullagerfabriken (SKF)], and a portable laptop, as shown in Fig. 6. According to previous technical experience, the setting of the sampling window, sampling frequency, and the cutoff frequency of the vibration analyzer is referred to [28]. The vibration acceleration signals of the harmonic drives are collected by three sensors installed in orthogonal directions.

During the testing process of the vibration experiment, except for the fifth axis, the other axes of the industrial robot are locked and do not move. The motor on the robot drives the harmonic drive through the belt to realize the movement of the mechanical arm. The fifth joint was used

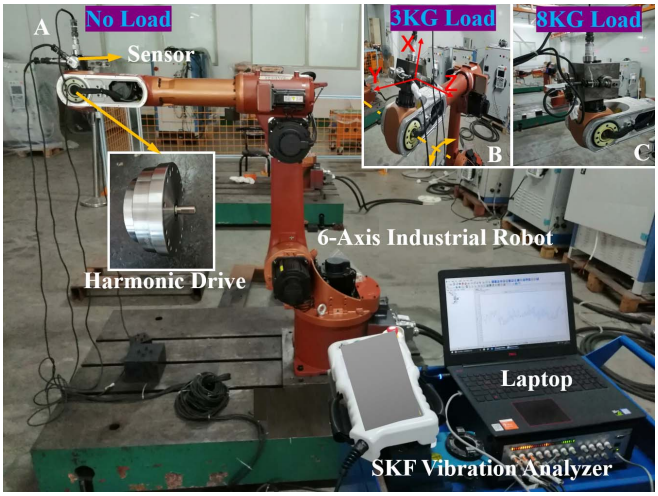

Fig. 6. Industrial robot vibration test experimental bench.

TABLE I
Explanation of the Health Status of Harmonic Drive

Class Label	Description of various health status signals
0	Normal and noise <78db under various working conditions
1	Jitter and noise>78db under 0kg&H speed condition
2	Jitter and noise>78db under 3kg&H speed condition
3	Jitter and noise>78db under 8kg&H speed condition
4	Severe jitter and noise>78db under 0kg&S speed condition
5	Jitter and noise>78db under 3kg&M speed condition
6	Jitter and noise>78db under 3kg&S speed condition

to reciprocate between $-105°$ and $+105°$ angles. There are three kinds of payloads (0, 3 kg, and 8 kg) and four kinds of test speeds (1247(L), 2492(M), 3739(H), and 4985(S) r/min). The reduction ratios of the fifth axis transmission chain and the harmonic drive are 84.1666 and 100, respectively. The vibration signals collected under these 12 test conditions are used for subsequent fault diagnosis.

B. Spectrum Dataset Construction

First, overlap and sample the collected original vibration acceleration signals by moving a fixed sampling window to expand a series of real sample units of various health statuses. The number of expanded samples of the vibration acceleration signal will be four times the original number. Second, use FFT to process each data sample unit sequentially to obtain the dataset that was used to form a real dataset. The length of the original sample used for FFT analysis is 6142, which includes all data of one movement cycle of the harmonic drive. These fault samples will be used for subsequent GAN training to generate data to build a balanced dataset. Vibration and noise are important criteria for evaluating whether a harmonic drive is operating normally. The failure of the harmonic drive occurs in these 12 test conditions, and the occurrence of the failure is related to the operating conditions. Therefore, the collected various health status signals are labeled, as shown in Table I.

Besides, the dataset composed of the data collected by three vibration acceleration sensors includes 12 test conditions.

TABLE II
NETWORK PARAMETERS OF THE GAN-DSM-MSCNN

Layer name	GAN-DSM-MSCNN
Generator	
Input Size	G_in = Input(shape=[10])
Fc1	out features=200, activation: tanh
Fc2	out features=3072, activation: tanh
Discriminator	
Input Size	D_in = Input(shape=[3072])
Reshape	Output Shape=(3072, 1)
Conv1	Output Shape=(3068, 50), Param: 300
Dropout	Output Shape=(3068, 50), drate=0.25, leak=0.2
Fc1	Linear(in_channels=153400,out_channels=50)
Fc2	Sigmoid(in_channels=50,out_channels=2, Param:102)
Fault Classifier (MSCNN)	
MS Layer	[3072 1536 1024 716]
Input Size	46x46x3
Conv1	Conv2d(in=3,out=12, kernel size=5,stride=1,padding=2)
Pooling1	Kernel size=2
Conv2	Conv2d(in=12,out=16,kernel size=5,stride=1,padding=2)
Pooling2	Kernel size=2
Fc1	Linear(in_channels=1024, out_channels=512,bias=True)
Fc2	Linear(in_channels=512, out_channels=80,bias=True)
Output	Linear(in_channels=80, out_channels=7,bias=True)

The naming of each dataset is composed of load, speed, harmonic drive number, and sensor number in sequential order. These datasets will be used for subsequent multiclassification. For example, the ZeroMA3_2 dataset denotes the acceleration vibration data collected by the second sensor of the third harmonic drive under no-load and *M* speed working conditions.

C. Parameters Selection of Network Structure

The parameters of the network are given in Table II, which are determined by empirical values and a series of debugging experiments. Besides, the SNR value of Gaussian noise is 20. The generator of GAN contains two fully connected layers. The excitation function is tangent hyperbolic (Tanh), and the loss function is stochastic gradient descent (SGD). Moreover, the discriminator of GAN includes a convolutional layer and two fully connected layers. The kernel size, the loss value, and the step size of the convolutional layer are 5, 0.25, and 1, respectively. The learning rate of the network is 0.001. The rectified linear unit (Relu) and sigmoid are selected as the excitation functions of the convolutional layer and the fully connected layer, respectively. Finally, the MSCNN classifier used for fault diagnosis contains two pairs of convolutional layers and pooling layers, and three fully connected layers. The kernel size, step size, and padding value of the convolutional layer are 5, 1, and 2, respectively. Besides, the kernel size and the step size of the pooling layer are both 2. The selection of optimizer is Adam and cross-entropy is chosen as the loss function.

The development environment is as follows: CPU: Intel Core i7-9750H at 2.60 GHz*12, GPU: NVIDIA GeForce GTX 1660 TI, Memory: 16 G, and Python 3.7.

TABLE III
SPECTRUM OF HARMONIC DRIVE UNDER 12 TESTING CONDITIONS

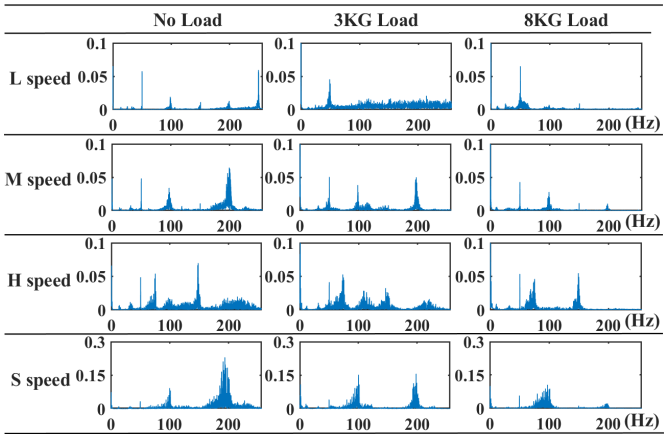

IV. RESULTS AND DISCUSSION

A. Spectrum Results of Harmonic Drive

In this section, the frequency spectrum of the harmonic drive under 12 test working conditions can effectively reflect the features of the vibration signal, which is given in Table III.

Manufacturing errors and assembly errors are the main reasons that cause abnormal vibration of the harmonic drive under certain operating conditions, which are different from conventional gearboxes and other transmission devices. It can be seen from Table III that at the same speed, the spectrum amplitude of the no-load condition is larger than that of the 3 and 8 kg conditions, which means that the vibration is more severe under certain working conditions. Besides, under the same load, the greater the operating speed, the greater the spectrum amplitude of the vibration signal, which means the greater the vibration energy. Although the fault characteristics of the harmonic drive can be revealed through the spectrum, it is not enough to effectively diagnose the harmonic drive under multiple working conditions and scarce fault data. According to the statistical data provided by the manufacturer, failures are most likely to occur under no-load and *S* speed conditions, and failures are distributed under different working conditions. To further diagnose the fault of the harmonic drive, the GAN technique will be used in Section IV-B to obtain the analysis results.

B. Results of GANs

To visually display the training process of generated data under different epochs of the GANs, the loss of the discriminator and generator using ZeroMA5_3 dataset were illustrated in Fig. 7. It can indirectly reflect the data quality of the 1-D spectrum obtained by the generative network. The generators and discriminators in the network are continuously optimized during the generation process and learn how to be better than the other. Therefore, either the generator or the discriminator is lowering its loss relative to a loss gain on the other side until both reach convergence. Generally, the value of the discriminative loss will be small and close to 0, which means

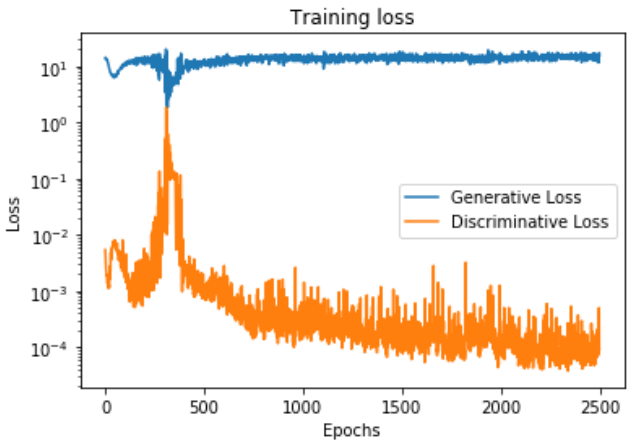

Fig. 7. Loss value of the GAN for ZeroMA5_3 sample generation.

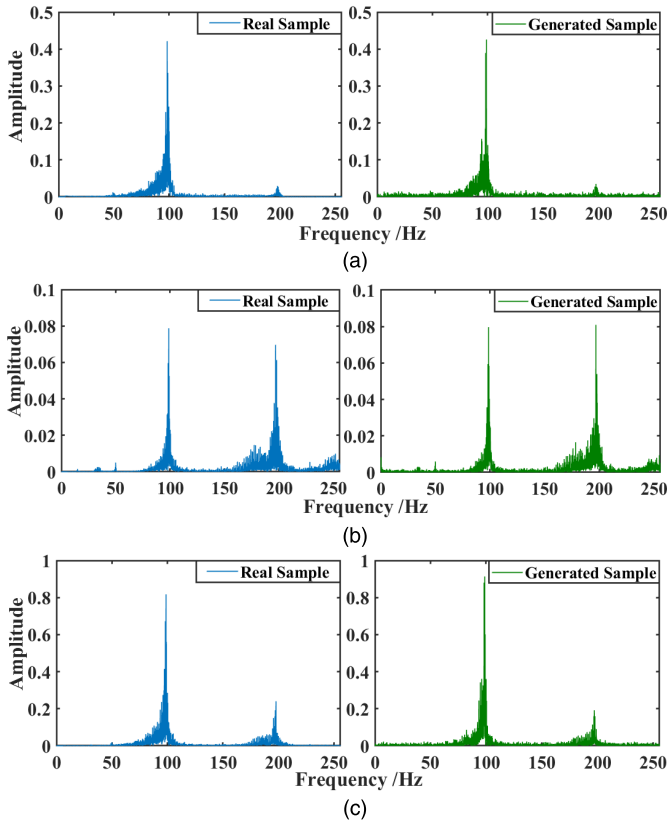

Fig. 8. Real and generated spectrum of the vibration acceleration signal. (a) Normal condition (ZeroMA2_3). (b) Fault 2 (ZeroMA5_2). (c) Fault 3 (ZeroMA5_3).

better learning ability. Besides, the larger the epochs, the more training time is required.

Besides, detailed observations of the data generated by the network model are given and compared with real data. The real spectrum and generated spectrum of various vibration acceleration signals of the harmonic drive under different working conditions are shown in Fig. 8, which can effectively reflect the comprehensive fault characteristics of the time domain vibration signal.

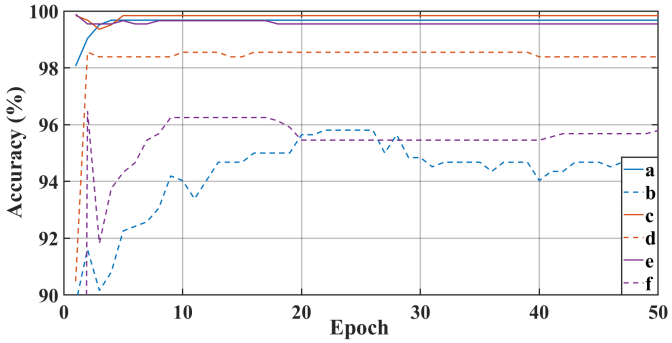

Fig. 9. Test accuracy in different real datasets. (a) Train the generated data, test the real data (added noise data). (b) Train the real data, test the real data (added noise data). (c) Train the generated data, test the real data (extended data). (d) Train the real data, test the real data (extended data). (e) Train the generated data, test the real data (added noise data and extended data). (f) Train the real data, test the real data (added noise data and extended data).

It can be observed from Fig. 8 that the generated spectrums are close to the real spectrums under normal or abnormal working conditions, which indicates that the generated spectrums have captured the basic distribution characteristics of the real signal. Besides, the real spectrum and the generated spectrum also have differences. The collected real signals are often mixed with noise, but the generated spectrum data contains useful components of real data, which can be used to expand the original data distribution.

C. Multiclassification Results of Harmonic Drive

1) Effects of Generated Data: ZeroMA2_2, ZeroMA9_2, ZeroMA3_2, and ZeroMA5_2 datasets were used to evaluate the effect of the generated data. The number of each category of failure sample both in the training datasets and the test datasets is 100 in this experiment. First, the real data of different products under the same working conditions were expanded in the test dataset. Besides, the Gaussian noise was used to simulate the interference of the real environment and be added to the original data. Second, the filtered high-quality generated dataset and real dataset were used to train the network and then compare the test accuracies of the remaining three sets of different real datasets. The testing accuracies in different real testing datasets are given in Fig. 9.

The differences between curve a and b, curve c and d, and curve e and f are that the filtered high-quality generated dataset use generated data to train, while the real dataset uses real data to train. Fig. 9 presents the convergence test accuracy of a, c, and e datasets that are 99.68%, 99.84%, and 99.55%, respectively, while the convergence test accuracy of b, d, and f datasets are 94.68%, 98.39%, and 95.80%. This effectively verifies that the generated data is more representative of the true distribution than that of real data, which helps to improve the multiclassification accuracy.

To avoid the adverse impact of scarce fault samples and data imbalance of various categories of fault samples of harmonic drive, the high-quality generated samples obtained by GAN-DSM were added to the training dataset in this experiment. Therefore, 10% of the generated samples were

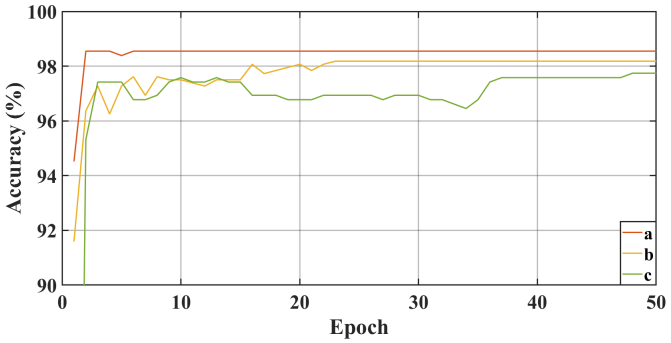

Fig. 10. Test accuracy in different real datasets. (a) Test on real data (added noise data). (b) Test on real data (expanded data). (c) Test on real data (added noise data and expanded data).

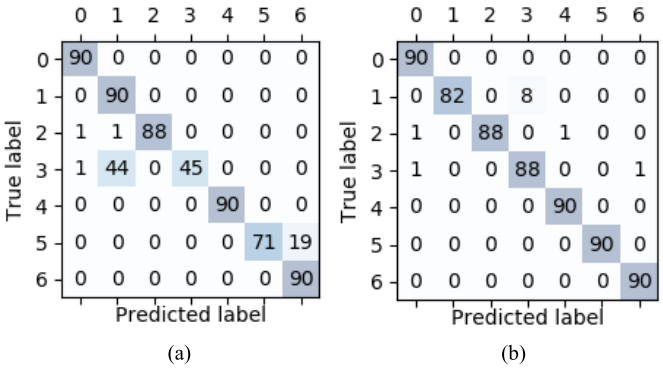

Fig. 11. Train in different datasets and test in real datasets (add noise and expand data). (a) Training in real data. (b) Training in generated data.

added to the original real dataset, and then they were mixed as the training dataset, and the classification performance of three different real testing datasets are further compared, as shown in Fig. 10.

The convergence accuracies obtained on the real test datasets *a*, *b*, and *c* are 97.74%, 98.55%, and 98.18%, respectively, as shown in Fig. 10. Besides, Figs. 9 and 10 show that the classification performance test on real data with expanded data is better than real data with added noise data and expanded data, and the latter is better than the real data with added noise data. By comparing Figs. 9 and 10, it shows that using a mixed dataset with real samples and generated samples for training, the test accuracies obtained in the three real testing datasets are all higher than that only using the limited amount of real training samples. Furthermore, only using generated samples for training can obtain the best classification performance. Therefore, the results imply that the generated data created by GANs can effectively not only capture the useful fault features of real data but also that the generated data can improve the multiclassification accuracy of fault diagnosis when they were added to the real imbalanced training dataset.

2) Results of Multiclassification: To vividly show the effect of the generated data of GAN, we compare the multiclassification results of the harmonic drive health status when using real datasets or generated datasets for training. The datasets used in the experiment consist of ZeroMA3_1, ZeroMA5_1, ZeroMA5_2, ZeroMA5_3, ZeroMA4_1, ZeroMA4_2, and ZeroMA4_3. The ratio of the number of data used for network training and testing is 7:3. There are seven categories, including one normal and six faults. The number of test samples in each category is 90. The real and generated dataset was used to train, then the classification accuracy of the remaining real test samples is shown in Fig. 11.

The confusion matrix is usually used to visually indicate the number of accurate predictions and the number of misclassifications for each category in the test result. Label 0 represents the normal state and labels 1–6 represent six categories of fault states. It indicates that the testing accuracy of each category in Fig. 11(a) is 1, 1, 0.98, 0.50, 1, 0.79, and 1, respectively, and the overall accuracy is 0.90, while the accuracy of each category in Fig. 11(b) is 1, 0.91, 0.98, 0.98, 1, 1, and 1, respectively, and the overall accuracy is 0.98. Therefore, the above results show that using the generated data to classify each category is usually better than using actual data, and the accuracy of the overall test classification is also higher.

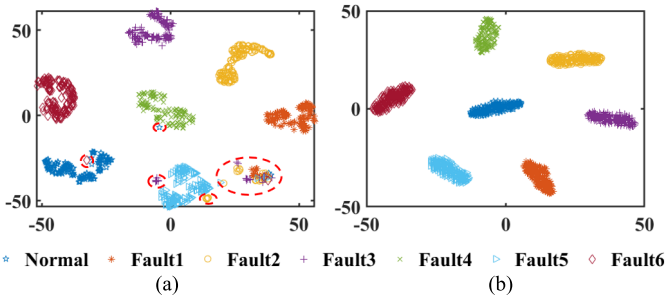

Fig. 12. Feature visualization of seven health statuses through the t-SNE technique. (a) All categories are real data. (b) All categories are generated data.

3) Results of Robustness Analysis: The amount of real fault data is scarce, and these signals always contain many interference components. However, GANs can use to augment the real training dataset by generating various categories and different numbers of high-quality fault samples.

To obtain robustness analysis for generated fault data and visually display the clustering effect of various categories of fault data, t-distributed stochastic neighbor embedding (t-SNE) [29] was used to reduce the dimensionality of the vibration spectrum of the harmonic drive under seven healthy statuses and map them to a 2-D space, as given in Fig. 12.

In Fig. 12(a), the misclassified samples are circled with red dotted lines. Compared with using the same number of real samples, the clustering effect of the generated data obtained by the proposed method is better, and the data between different categories are more separated from each other, as shown in Fig. 12(b). Although the real sampled signal is coupled with the interference of the external electromechanical system, the generated sample can effectively represent the useful features of the original signal. Therefore, it indicates the generated data have more realistic distribution characteristics and have a good antinoise effect to improve the classification performance.

TABLE IV
AVERAGE TESTING ACCURACIES OF HARMONIC DRIVE FOR DIFFERENT IMBALANCE RATIO (%)

Method	10:1	10:1 (-N)	20:1	20:1 (-N)	40:1	40:1 (-N)	70:1	70:1 (-N)
Un-processed	89.68	86.98	85.56	78.57	85.40	72.53	71.43	71.11
Under-sampling	92.38	89.37	86.67	83.02	85.55	79.21	83.81	72.86
Over-sampling	94.60	90.16	93.33	88.89	92.86	87.78	87.30	82.70
SMOTE	85.71	78.10	85.56	77.62	85.39	76.03	83.49	75.24
ADASYN	87.62	78.25	85.71	77.94	85.24	74.29	83.33	73.65
GAN	95.87	93.97	96.51	94.44	96.98	92.22	96.67	94.29
GAN-DSM	**98.89**	**98.10**	**99.19**	**98.41**	**99.37**	**98.73**	**99.52**	**99.12**

D. Comparison of Different Fault Diagnosis Methods

Imbalanced data will hurt the results of multiclassification, it is necessary to take various data augmentation methods to balance the scarce fault data of each category. Therefore, the complex multiclassification of imbalances between different health conditions will be discussed. By default, there are seven categories (including one normal category and six abnormal categories) in the training dataset, and each category has 210 samples. The training samples of the normal category are all real. Each category of fault data in the training set includes real data and generated data, and the number of real data among them is determined by the imbalance ratio. Besides, each category contains 90 real samples in the test dataset. Different data augmentation methods were used to balance each category of the training dataset, and then the same classifier was used to obtain the average testing accuracies by five trials, as shown in Table IV. "$-N$" means that the original signal is mixed with Gaussian noise such that the SNR is 20.

Table IV shows that the effect of the undersampling is worse than that of the oversampling, and the interference of noise will reduce the accuracy of the test classification. Besides, compared with other traditional data augmentation methods, GAN can achieve better performance and robustness with relatively small fluctuations. Furthermore, the proposed GAN-DSM method with a DSM can obtain the best fault diagnosis results, which can select the high-quality generated data from the randomly generated samples of the GANs. Besides, as the number of generated samples added to the training set increases, the fault diagnosis performance of the harmonic drive will be better. This shows that GAN-DSM can create and select meaningful samples to construct the balanced datasets for training. Moreover, the fault diagnosis performance of the harmonic drive can be effectively improved under the condition of imbalanced fault data.

Furthermore, we use different network models to compare the fault diagnosis results of the harmonic drive and the imbalance ratio is 10:1. The average testing accuracy obtained by five repeated experiments is shown in Table V.

TABLE V
TESTING AVERAGE ACCURACIES OF DIFFERENT METHODS IN IMBALANCED FAULT DIAGNOSIS

Methods	Average testing accuracies (%)	
	10:1	10:1(-N)
MMN-FC [12]	85.71	77.62
MobileNetV2-FC [30]	91.43	87.46
GoogLeNet-FC [30]	89.68	88.57
ResNext50_32x4d-FC [30]	87.30	84.84
DenseNet-121-FC [30]	90.79	86.51
EfficientNet-B0-FC [30]	93.73	89.01
Conditional GAN [21]	88.97	85.08
MUNIT [23]	92.07	86.24

The MNN-FC contains a spatial multiscale feature module and a focal loss function. MobileNetV2 pretrained model is a lightweight network. GoogLeNet pretrained model maintains the sparsity of the neural network structure through the modular structure of Inception. ResNext50_32 $\times$ 4d pretrained model contains 50 layers, it can reduce the number of hyperparameters through the topology of the submodule. DenseNet-121 pretrained model uses Dense connections, which can resist over-fitting and has a stronger generalization ability. EfficientNet-B0 pretrained model utilizes composite coefficients to uniformly scale all dimensions of the model, which can improve accuracy and efficiency. In addition, contemporary multimodal GANs including conditional GAN and multimodal unsupervised image-to-image translation (MUNIT) are also used to generate different categories of fault data at the same time and then compare the fault diagnosis results separately. Although proper loss function or network model can help improve the fault diagnosis performance under data imbalance, various categories of extremely scarce fault data will still adversely affect the results without data augmentation. Therefore, it is difficult to obtain ideal results through the above methods without effectively augmenting the various categories of imbalanced fault data of the harmonic drive.

E. Contrast Results of Different Classifiers

After using different data augmentation methods to balance the scarce fault data, various machine learning algorithms are used as classifiers for harmonic drive fault diagnosis. However, the choice of a classifier is critical because it directly affects the results of the classification. Therefore, the scikit learn library [31] is used to import different algorithm modules, such as support vector machine (SVM), decision tree (DT), and K-nearest neighbor (KNN). Besides, the classic CNN and the proposed MSCNN classifiers were selected to compare the testing accuracy, respectively. Finally, five repeated test experiments were performed to obtain the comparative results given in Table VI.

Table VI shows that the multiclassification performance of MSCNN for fault diagnosis is better than other machine learning classifiers. The constructed MSCNN has the ability to

TABLE VI
TEST ACCURACY AND TIME COST OF HARMONIC DRIVE UNDER VARIOUS CLASSIFIERS

Method	Testing accuracy (%)		Time cost (s)	
	Mean	Variance	Mean	Variance
GAN-DSM-MSCNN	**98.49**	**1.02**	**114.97**	**1.25**
GAN-MSCNN	96.35	1.43	116.53	1.57
GAN-CNN	93.29	1.13	117.22	5.87
GAN-SVM	71.43	0.06	18.95	0.05
GAN-DT	64.23	0.64	7.60	0.17
GAN-KNN	76.98	0.01	8.82	0.48

enhance the fault diagnosis of the harmonic drive, which can effectively capture the multiscale features of input samples. Besides, the combination of the GAN-DSM generative model and the MSCNN classifier can achieve the best results, and the accuracy fluctuations are small, which also proves that the generated data selected by the proposed DSM and multiscale processing modules are beneficial to improve the overall fault diagnosis performance.

V. DISCUSSION AND CONCLUSION

In this article, we propose an intelligent diagnosis architecture (GAN-DSM-MSCNN), which uses multiple GANs to generate various types of fault data to avoid the adverse effects of imbalanced health status data of harmonic drive on the diagnosis results. The DSM (including data filtering and data purification) is designed to select the high-quality generated data, which is used to expand and balanced the training datasets. Besides, MSCNN is used to capture the multiscale features of the vibration signal and improve the fault multiclassification accuracy of the harmonic drive. The contrast experiments show that GAN-DSM-MSCNN not only can solve the problem of imbalanced health status data by generating meaningful new fault data but also can obtain better fault diagnosis results than other methods.

In addition, the limitations of this article can be summarized in the following three aspects.

1) To design a custom loss function for the proposed model rather than simply use the cross-entropy loss, further exploration is needed taking into account the imbalanced ratio of different categories of fault samples and simultaneously combine the DSM to constraint the generated data of each epoch.
2) Multiple GANs are used to generate each category of fault data separately, which will consume much computing resources. Moreover, the overall framework needs to train GANs and MSCNN separately which is also inefficient in industrial applications. It is necessary to avoid the network being too complex and bloated, and to ensure the quality of various categories of generated fault data.
3) To get better model debugging parameters, methods such as particle swarm optimization (PSO) and other algorithms are needed to employ.

In the future, we will simultaneously optimize the network structure of multiple-GANs to reduce computational resources and improve training efficiency and combine transfer learning to achieve cross-domain fault diagnosis of the harmonic drive.

REFERENCES

[1] T. D. Tuttle, "Understanding and modeling the behavior of a harmonic drive gear transmission," Massachusetts Inst. Technol., Cambridge Artif. Intell. Lab., Cambridge, MA, USA, Tech. Rep. AI-TR-1365, 1992.

[2] I.-G. Park, I.-K. Kim, and M.-G. Kim, "Vibrational characteristics of developed harmonic reduction gear and fault diagnosis by Campbell diagram," in *Proc. 15th Int. Conf. Control, Autom. Syst. (ICCAS)*, Oct. 2015, pp. 2062–2065.

[3] C. Adams, A. Skowronek, J. Bös, and T. Melz, "Vibrations of elliptically shaped bearings in strain wave gearings," *J. Vibrat. Acoust.*, vol. 138, no. 2, Apr. 2016, Art. no. 021004.

[4] Y. Guo, X. Zhao, W.-B. Shangguan, W. Li, H. Lü, and C. Zhang, "Fault characteristic frequency analysis of elliptically shaped bearing," *Measurement*, vol. 155, Apr. 2020, Art. no. 107544.

[5] J. Zheng and W. Yang, "Failure analysis of a flexspline of harmonic gear drive in STC industrial robot: Microstructure and stress distribution," *IOP Conf. Ser., Mater. Sci. Eng.*, vol. 452, no. 4, Dec. 2018, Art. no. 042148.

[6] F. Jia, Y. Lei, J. Lin, X. Zhou, and N. Lu, "Deep neural networks: A promising tool for fault characteristic mining and intelligent diagnosis of rotating machinery with massive data," *Mech. Syst. Signal Process.*, vols. 72–73, pp. 303–315, May 2016.

[7] X. Guo, L. Chen, and C. Shen, "Hierarchical adaptive deep convolution neural network and its application to bearing fault diagnosis," *Measurement*, vol. 93, pp. 490–502, Nov. 2016.

[8] H. Liu, J. Zhou, Y. Zheng, W. Jiang, and Y. Zhang, "Fault diagnosis of rolling bearings with recurrent neural network-based autoencoders," *ISA Trans.*, vol. 77, pp. 167–178, Jun. 2018.

[9] W. Qiao and D. Lu, "A survey on wind turbine condition monitoring and fault diagnosis—Part II: Signals and signal processing methods," *IEEE Trans. Ind. Electron.*, vol. 62, no. 10, pp. 6546–6557, Oct. 2015.

[10] Y. Sun, A. K. Wong, and M. S. Kamel, "Classification of imbalanced data: A review," *Int. J. Pattern Recognit. Artif. Intell.*, vol. 23, no. 4, pp. 687–719, 2009.

[11] S. G. A. Fernández, *Learning from Imbalanced Data Sets*. Cham, Switzerland: Springer, 2018.

[12] Q. He, Y. Pang, G. Jiang, and P. Xie, "A spatio-temporal multiscale neural network approach for wind turbine fault diagnosis with imbalanced SCADA data," *IEEE Trans. Ind. Informat.*, early access, Nov. 27, 2020, doi: 10.1109/TII.2020.3041114.

[13] W. W. Y. Ng, J. Zhang, C. S. Lai, W. Pedrycz, L. L. Lai, and X. Wang, "Cost-sensitive weighting and imbalance-reversed bagging for streaming imbalanced and concept drifting in electricity pricing classification," *IEEE Trans. Ind. Informat.*, vol. 15, no. 3, pp. 1588–1597, Mar. 2019, doi: 10.1109/TII.2018.2850930.

[14] S. Lei, H. Zhang, K. Wang, and Z. Su, "How training data affect the accuracy and robustness of neural networks for image classification," in *Proc. Int. Conf. Learn. Represent. (ICLR)*, 2019.

[15] V. López, A. Fernández, S. García, V. Palade, and F. Herrera, "An insight into classification with imbalanced data: Empirical results and current trends on using data intrinsic characteristics," *Inf. Sci.*, vol. 250, pp. 113–141, Nov. 2013.

[16] H. Han, W. Y. Wang, and B. H. Mao, "Borderline-SMOTE: A new over-sampling method in imbalanced data sets learning," in *Advances in Intelligent Computing*, D. S. Huang, X. P. Zhang, G. B. Huang, Eds. Berlin, Germany: Springer, 2005, pp. 878–887.

[17] H. He, Y. Bai, E. A. Garcia, and S. Li, "ADASYN: Adaptive synthetic sampling approach for imbalanced learning," in *Proc. IEEE Int. Joint Conf. Neural Netw.*, Jun. 2008, no. 3, pp. 1322–1328.

[18] H. A. Gameng, B. B. Gerardo, and R. P. Medina, "Modified adaptive synthetic SMOTE to improve classification performance in imbalanced datasets," in *Proc. IEEE 6th Int. Conf. Eng. Technol. Appl. Sci. (ICETAS)*, Lumpur, Malaysia, Dec. 2019, pp. 1–5.

[19] Z. Zheng, L. Zheng, and Y. Yang, "Unlabeled samples generated by GAN improve the person re-identification baseline *in vitro*," 2017, *arXiv:1701.07717*. https://arxiv.org/abs/1701.07717

[20] Y. O. Lee, J. Jo, and J. Hwang, "Application of deep neural network and generative adversarial network to industrial maintenance: A case study of induction motor fault detection," in *Proc. IEEE Int. Conf. Big Data (Big Data)*, Dec. 2017, pp. 3248–3253.

[21] G. Douzas and F. Bacao, "Effective data generation for imbalanced learning using conditional generative adversarial networks," *Expert Syst. Appl.*, vol. 91, pp. 464–471, Jan. 2018.
[22] S. Shao, P. Wang, and R. Yan, "Generative adversarial networks for data augmentation in machine fault diagnosis," *Comput. Ind.*, vol. 106, pp. 85–93, Apr. 2019.
[23] X. Huang, M. Y. Liu, S. Belongie, and J. Kautz, "Multimodal unsupervised image-to-image translation," in *Computer Vision—ECCV* (Lecture Notes in Computer Science), vol. 11207, V. Ferrari, M. Hebert, C. Sminchisescu, Y. Weiss, Eds. Cham, Switzerland: Springer, 2018, pp. 179–196, doi: 10.1007/978-3-030-01219-9_11.
[24] W. Zhang, X. Li, X.-D. Jia, H. Ma, Z. Luo, and X. Li, "Machinery fault diagnosis with imbalanced data using deep generative adversarial networks," *Measurement*, vol. 152, Feb. 2020, Art. no. 107377.
[25] S. Barratt and R. Sharma, "A note on the inception score," 2018, *arXiv:1801.01973*. [Online]. Available: http://arxiv.org/abs/1801.01973
[26] X. Jiang and Z. Ge, "Data augmentation classifier for imbalanced fault classification," *IEEE Trans. Autom. Sci. Eng.*, early access, Jun. 11, 2020, doi: 10.1109/TASE.2020.2998467.
[27] A. K. Jain, "Data clustering: 50 years beyond K-means," *Pattern Recognit. Lett.*, vol. 31, no. 8, pp. 651–666, Jun. 2010.
[28] G. Yang, Y. Zhong, L. Yang, and R. Du, "Fault detection of harmonic drive using multiscale convolutional neural network," *IEEE Trans. Instrum. Meas.*, vol. 70, 2021, Art. no. 3502411, doi: 10.1109/TIM.2020.3024355.
[29] N. Pezzotti, B. P. F. Lelieveldt, L. V. D. Maaten, T. Hollt, E. Eisemann, and A. Vilanova, "Approximated and user steerable tSNE for progressive visual analytics," *IEEE Trans. Vis. Comput. Graphics*, vol. 23, no. 7, pp. 1739–1752, Jul. 2017.
[30] M. Tan and Q. V. Le, "EfficientNet: Rethinking model scaling for convolutional neural networks," 2019, *arXiv:1905.11946*. [Online]. Available: http://arxiv.org/abs/1905.11946
[31] *Scikit-Learn Library*. Accessed: Jan. 14, 2020. [Online]. Available: https://scikit-learn.org/stable/

Guo Yang received the M.S. degree in mechanical engineering from the Guangdong University of Technology, Guangzhou, China, in 2018. He is currently pursuing the Ph.D. degree with the Shien-Ming Wu School of Intelligent Engineering, South China University of Technology, Guangzhou.

His main research focuses on intelligent monitoring, diagnosis, and control of advanced manufacturing systems.

Yong Zhong (Member, IEEE) received the B.Eng. degree in mechanical design, manufacturing, and automation from the Huazhong University of Science and Technology, Wuhan, China, in 2011, the M.Eng. degree in control engineering from the University of Chinese Academy of Sciences, Beijing, China, in 2014, and the Ph.D. degree in mechanical and automation engineering from The Chinese University of Hong Kong, Hong Kong, in 2017.

He was a Research Fellow with the National University of Singapore, Singapore, from 2017 to 2019. He is currently an Assistant Professor with the Shien-Ming Wu School of Intelligent Engineering, South China University of Technology, Guangzhou, China. His research interests include bioinspired robots, soft robots, and intelligent diagnosis and control.

Lie Yang received the B.Eng. degree in mechanical design, manufacturing, and automation from the School of Mechanical Engineering, Wuhan Polytechnic University, Wuhan, China, in 2015. He is currently pursuing the Ph.D. degree with the Shien-Ming Wu School of Intelligent Engineering, South China University of Technology, Guangzhou, China.

His main research focuses on artificial intelligence, computer vision, and electroencephalogram decoding.

Hui Tao received the M.S. degree in control theory and control engineering from the Wuhan University of Science and Technology, Wuhan, China, in 2011. He is currently pursuing the Ph.D. degree with the Shien-Ming Wu School of Intelligent Engineering, South China University of Technology, Guangzhou, China.

He also works with the National and Local Joint Engineering Research Center for Industrial Friction and Lubrication Technology, Guangzhou. His main research focuses on intelligent monitoring, diagnosis, and control.

Jianying Li received the M.S. degree in safety technology and engineering and the Ph.D. degree in mechanical design and theory from the South China University of Technology, Guangzhou, China, in 2010 and 2016, respectively.

He was the Safety Engineer with Guangzhou CNC Equipment Company from 2010 to 2013, in charge of equipment safety and safe production. He is currently a Lecturer with the School of Mechanical and Automotive Engineering, Zhaoqing University, Zhaoqing, China. His main research focuses on vehicle dynamics, robot design, and control.

Ruxu Du received the M.S. degree in automatic control from the South China University of Technology, Guangzhou, China, in 1983, and the Ph.D. degree in mechanical engineering from the University of Michigan, Ann Arbor, MI, USA, in 1989.

From 1991 to 2001, he taught at the University of Windsor, Windsor, ON, Canada, the University of Miami, Coral Gables, FL, USA, and The Chinese University of Hong Kong (CUHK), Hong Kong, where he has been a Professor with the Department of Mechanical and Automation Engineering and the Director of the Institute of Precision Engineering, since 2002. He is currently a Professor with the Shien-Ming Wu School of Intelligent Engineering, South China University of Technology. His research interests include precision engineering, condition monitoring, fault diagnosis, manufacturing processes (metal forming, machining, plastic injection molding, etc.), and robotics.

Dr. Du became a fellow of the America Society of Mechanical Engineers (ASME) in 2009, the Society of Manufacturing Engineers (SME), and the Hong Kong Institute of Engineers (HKIE) in 2012, and an Academician of Canadian Academy of Engineering in 2017.